

# The Metastable State of Fermi-Pasta-Ulam-Tsingou Models

Kevin A. Reiss

Senior Honors Thesis

Advisor: Professor David K. Campbell



Physics Department

Boston University

May 4, 2022

## CONTENTS

Abstract	3
Acknowledgements	4
I. Introduction	7
II. Methods	9
A. Models	9
B. Numerical Methods	11
C. Spectral Entropy	12
III. Phenomena	13
A. FPUT Recurrences	13
B. Metastable State	15
IV. $\alpha$ -FPUT Model	18
A. Strength of FPUT Recurrences	18
B. Lifetime of Metastable State	22
1. Procedure	22
2. Analysis	25
C. Spectrum	29
V. $\beta$ -FPUT model	31
A. Comparison Between $\beta > 0$ and $\beta < 0$	31
B. Lifetime of Metastable State	33
VI. Conclusion	35
References	36

## ABSTRACT

Classical statistical mechanics has long relied on assumptions like the equipartition theorem to solve complicated systems of many particles. The successes of this approach are many, but there are also many well-known issues with classical theories for which the introduction of quantum mechanics is necessary, e.g. the ultraviolet catastrophe. However, more recently, the validity of assumptions like this have been called into question. A more careful analysis of a simplified model for blackbody radiation was able to elicit the Stefan-Boltzmann law using purely classical statistical mechanics [4]. The novel approach was a careful analysis of a “metastable” state which delays the approach to equilibrium.

In this thesis we perform a broad analysis of the metastable state in the  $\alpha$ -FPUT and  $\beta$ -FPUT models, both quantitative and qualitative. We start with a visualization of the metastable using spectral entropy ( $\eta$ ). This single degree of freedom has the power to quantify the distance to equipartition. A comparison to the integrable Toda model allows us to define the lifetime of the metastable state.

We visualize the strength of recurrences in the  $\alpha$ -FPUT model, yielding the surprising result that the recurrence strength is a function only of the essential system parameter  $R = (N + 1)^{3/2} \sqrt{E\alpha^2}$  for the  $\alpha$ -FPUT model. We devise a method to measure the lifetime of the metastable state  $t_m$  in the  $\alpha$ -FPUT model. Our procedure involves averaging over random initial phases in the  $P_1$ - $Q_1$  plane. This bin average provides a relevant length distance, the standard deviation, from which we then determine when the  $\alpha$ -FPUT model trajectories break off from the entropy of the Toda model. Applying this procedure gives us a power law scaling for  $t_m$ , with the surprising result that the power laws for different system sizes collapse down to the same exponent as  $E\alpha^2 \rightarrow 0$ .

We explore the spectrum of the  $\alpha$ -FPUT model, compared to that of the Toda model. This analysis suggestively demonstrates a method for an irreversible energy dissipation process proven by Onorato et al. [40]: four-wave and six-wave resonances. These preliminary results appear to confirm the presence of these resonances, but more work is needed on the subject. A similar depiction is given for the  $\beta$ -FPUT model. We explore different behavior for the two different signs of  $\beta$ . Last, we describe a procedure for calculating  $t_m$  in the  $\beta$ -FPUT model, a very different task than for the  $\alpha$ -FPUT model since the  $\beta$ -FPUT model is not the truncation of an integrable model.

## ACKNOWLEDGEMENTS

My primary and utmost gratitude must be given to my advisor, David Campbell. David has been more than a thesis advisor for me, he is an academic advisor, a mentor, and the reason I decided to study physics in the first place. I may have entered BU as an engineering major, but I always had a passion for physics. Foolishly, I thought just a minor might be enough to satiate my curiosity, so I took just a couple physics classes my freshman year. That was, until I met David. I knocked on his door one day, a timid freshman with a scant resume in hand, searching for research opportunities. David took me in with open arms, and introduced me to an undergraduate working with him at the time, Sal Pace. Both of them were more than patient with me as I stumbled blindly into the world of academic research. Through my project with them I grew infinitely more confident, as a researcher, a student, and a human.

It became immediately clear that physics was my true calling, and pretty soon after I met him I was sitting in David's office, submitting my official intent to transfer colleges from ENG to CAS and get a major in physics. I felt immediately comfortable in this new community, thanks to David volunteering to serve as my academic advisor, and to Sal introducing me not only to the people in the department but also to the customs of the department like navigating the science building, using the tools of physics, and of course extracting the perfect cup of espresso.

While I look fondly on those glory days of scientific exploration, they would not last long, when the COVID-19 pandemic shuttered the doors of BU's research community and I found myself attempting to pursue my next project with David from the comfort of my childhood home in Connecticut. Trying to perform research without being able to meaningfully interact with my collaborators or anyone else in the department was extremely isolating for me, and my progress and motivation slumped precipitously. However, David was patient with me and understanding of the situation. He helped guide me to a shift in focus with an internship to replace the semester I had planned to spend abroad in Geneva. He was willing to let me pursue new avenues, while still keeping me involved in his research group and mentoring other students of his. The intention of this thesis is to essentially wrap up a lot of the work I did with David, put a pin in it all and declare victory over it despite the very extenuating circumstances it was performed under.

David was willing to let me take on whatever role made the most sense, and for some time that role was being a mentor for other students performing research with David: Jenebi, Matt, and more recently Kristen. These opportunities are very unique for an undergraduate, and wouldn't be possible without the incredible familiarity I have developed with the research subject matter, and David's group, all thanks to David's warm and welcoming guidance. David also introduced me to Mathematica, a program which soon became my passion and my forte. David has graciously written innumerable recommendation letters for me, which has played no small part in opening many doors to me. Most of what I am capable of doing is thanks to David, for which I am eternally grateful.

I already mentioned Sal Pace, because even a brief synopsis of my path at BU wouldn't be complete without him, but he deserves his own special acknowledgment. Sal dedicated an incredible amount of time to mentoring me, and quickly grew to be my close friend. He was integral in my introduction to physics, and he helped solidify my place in it. Sal pushed me to take harder classes that I wouldn't have known existed without him, and pushed me to apply for scholarships like the Goldwater scholarship, which quite frankly changed my life. The application process was arduous to say the least, and I'm not sure I could have gotten through it without Sal. He was always willing to sit down and review a section of my application to patiently and honestly suggest improvements. I've just barely scratched the surface of what Sal selflessly did for me, but if I tried to enumerate it all there wouldn't be room for my actual thesis.

I am grateful to all of the physics professors, many whom I've had the pleasure of taking a class with, and others whom I only know from seeing around the science building. I'm constantly astounded by the caliber and accomplishments of our incredible faculty. To name a few, Chris Laumann and Anushya Chandran taught some of the only fully-normal physics classes I took before COVID shuttered our classrooms. They have served as recommendation letter writers for me, mentors on occasion, and always have something interesting to talk about while we brew the next shot of espresso. I have only taken one class with Jim Rohlf, but he took me on as his Learning Assistant for PY405/406 in my junior year, which has been an incredible opportunity for me. Jim trusted me enough to let me help rewrite his class materials to better work with remote teaching, a project which firmly solidified my understanding of classical electrodynamics and also resulted in a published textbook between the two of us. Very few professors are willing to undertake such a large project

as this one with an undergraduate student, and I am very thankful to Jim for all of the experiences and opportunities he has provided me.

I have enjoyed my time in the physics department in no small part thanks to my friend Nik Gjonbalaj. Nik and my paths have been very similar in some regards, and it has been comforting and very helpful to have such a close friend in a lot of my classes. Our research interests were aligned for a little bit, and I appreciated working closely with someone who is one of my closest friends. Nik has pushed me to excel harder than I would on my own, and provided a helpful hand whenever I couldn't get there on my own.

Of course, the final acknowledgments go entirely to my parents. I quite literally would not be where I am today without them. They are always willing to let me go my own way when it's best for me, but are always more than happy to welcome me home with open arms. This was especially important for these last four years of college, where I spent much more time at home than I expected due to BU's campus being closed for large portions of my college career. Having a supportive home to go back to if I ever need it has enabled me to flourish. They are always suggesting opportunities for me to grow, but never forcing me to pursue any of them, instead guiding me gently. I am more than ever grateful to my parents for sending me to the college of my choice, and also for welcoming me home with arms open when that college closed down temporarily. They raised me to be the man I am today and I will always be striving to match the example they have set for me. To my parents, I love you and appreciate all of your guidance and every opportunity you have given me.

This is a far from exhaustive set of the people who have shaped my path through physics. There are many more people in my life who have given me more than I deserve and to whom I am also eternally grateful. I have been extremely blessed by the people in my life, and while my time at BU has not always been easy or straightforward, each and every one of you have made it more bearable and possible to get to where I am today.

Finally, I am grateful to UROP and BU-PRO for funding my research, along with SAEF for funding my travel to Chicago for the 2022 APS March Meeting.

## I. INTRODUCTION

Statistical mechanics, broadly speaking, aims to draw conclusions about the behavior of systems with large numbers of particles, without needing to solve the even larger number of equations that the particles obey. This approach has been successful in explaining anything from the temperature of a gas to the density of a neutron star, with many stunning discoveries in between [1]. One of the central tenets of this great field is the equipartition theorem [2], which assumes that over time, energy will be shared equally around the system. This assumption has led to many successes, e.g. the ideal gas law, but also some failures, e.g. the ultraviolet catastrophe from the failure of the Rayleigh-Jeans law to describe blackbody radiation [3]. Until recently, it was believed that the resolution of the ultraviolet catastrophe required the quantization of the energy of light into photons. However, more recently, an entirely classical resolution has been proposed [4]. By avoiding the assumption of the equipartition theorem, Wang et al. were able to find the Stefan-Boltzmann law through purely classical mechanics, consistent with the results of quantum mechanics. The key was the statistics of a quasi-stationary state in the model, which has the effect of stalling the approach to equilibrium. The impact of these new results on statistical mechanics and the approach to equilibrium remains to be seen.

In the early 1950s Enrico Fermi, John Pasta, Stanislaw Ulam and Mary Tsingou (FPUT) made the first detailed computational study of the validity of the equipartition theorem and instead found a similar quasi-stationary state [5]. Their assumption had been that adding even a small nonlinear term to the couplings between harmonic oscillators would allow the system to thermalize, i.e. reach a state of equipartition. However, they found that for small enough energies, the system would remain localized in mode space for all times which it was computationally possible to explore with their computer and that there were remarkable and entirely unexpected (near) recurrences to the initial state. This discovery opened the door for many important advances in the field of nonlinear dynamical systems: the discovery of solitons [6],  $q$ -breathers [7] and many more. Some of the most significant implications of their results were summarized on its 50-year anniversary [8]. The interested reader is directed towards these reviews of the FPUT problem: [9–12].

Our interest in this thesis is to computationally explore what is referred to as the “metastable state” [13] in the FPUT models. This is the quasi-stationary state which

stalls the approach to equipartition. In particular, we are interested in the lifetime of the metastable state, since the system is not able to approach equilibrium until the metastable state has ended. Understanding the lifetime of this state, especially any scaling laws that it exhibits, will provide a basis for analyzing systems with quasi-stationary states. It is our belief that the continued exploration of these states in physical systems has the potential to unlock more equivalencies between quantum mechanics and classical statistical mechanics, as was the case with blackbody radiation [4]. In particular, we will develop and explore some techniques which can help in standardizing the study of metastable states in non-integrable systems.

The structure of the thesis is as follows. First, we set up the systems we will explore in Section II. Then, in Section III we lay out the recurrence phenomenon and give an intuitive picture of the metastable state. In Section IV we explore the metastable state in the  $\alpha$ -FPUT model, the primary computational focus of our thesis. We explore the strength of recurrences (Section IV A), the lifetime of the metastable state (Section IV B), and the energy spectrum (Section IV C). Finally, we conclude with a more qualitative exploration of the metastable state in the  $\beta$ -FPUT model in Section V with a comparison between the two signs of  $\beta$  (Section V A) and a discussion of the possibility of measuring the lifetime of the metastable state in the  $\beta$  model (Section V B).

## II. METHODS

### A. Models

The general Hamiltonian for the systems we will consider is that of a chain of oscillators constrained to 1 dimension, whose nearest neighbor interactions are given by a potential  $V(r)$ , such that:

$$H(\mathbf{q}, \mathbf{p}) = \sum_{n=1}^N \frac{p_n^2}{2} + \sum_{n=0}^N V(q_{n+1} - q_n). \quad (1)$$

We will consider both the  $\alpha$ -FPUT model, with a cubic potential:

$$V_\alpha(r) = \frac{r^2}{2} + \frac{\alpha}{3}r^3, \quad (2)$$

and the  $\beta$ -FPUT model, with a quartic potential:

$$V_\beta(r) = \frac{r^2}{2} + \frac{\beta}{4}r^4, \quad (3)$$

with fixed boundary conditions  $q_0 = q_{N+1} = 0$  and  $p_0 = p_{N+1} = 0$  such that there are  $N$  distinguishable oscillators. The  $\beta$ -FPUT model can be considered as a perturbation of a linear chain of oscillators (with perturbation strength  $\beta$ ), while the  $\alpha$ -FPUT model behaves as a truncation of the Toda Lattice, which has potential energy:

$$V_{\text{Toda}}(r) = V_0 (e^{\lambda r} - 1 - \lambda r), \quad (4)$$

and has been shown to be integrable [14].

We define the normal modes through the canonical transformation:

$$\begin{bmatrix} q_n \\ p_n \end{bmatrix} = \sqrt{\frac{2}{N+1}} \sum_{k=1}^N \begin{bmatrix} Q_k \\ P_k \end{bmatrix} \sin\left(\frac{nk\pi}{N+1}\right). \quad (5)$$

These normal modes have frequencies:

$$\omega_k = 2 \sin\left(\frac{k\pi}{2(N+1)}\right). \quad (6)$$

This normal mode transformation diagonalizes the harmonic lattice (i.e.  $\alpha, \beta = 0$ ) but leaves off-diagonal terms in the Hamiltonians for the anharmonic models. These terms

lead to transfer of energy between modes. After this normal mode transformation the Hamiltonian for the  $\alpha$ -FPUT model is

$$H_\alpha(\mathbf{Q}, \mathbf{P}) = \sum_{k=1}^N \frac{P_k^2 + \omega_k^2 Q_k^2}{2} + \frac{\alpha}{3} \sum_{k,j,l=1}^N A_{k,j,l} Q_k Q_j Q_l \quad (7)$$

and for the  $\beta$ -FPUT model:

$$H_\beta(\mathbf{Q}, \mathbf{P}) = \sum_{k=1}^N \frac{P_k^2 + \omega_k^2 Q_k^2}{2} + \frac{\beta}{4} \sum_{i,j,l=1}^N B_{k,i,j,l} Q_k Q_i Q_j Q_l, \quad (8)$$

where the last summation term couples the normal modes together, allowing for energy sharing, with coupling constants [15, 16]:

$$A_{k,j,l} = \frac{\omega_k \omega_j \omega_l}{\sqrt{2(N+1)}} \sum_{\pm} [\delta_{k,\pm j \pm l} - \delta_{k \pm j \pm l, 2(N+1)}] \quad (9)$$

$$B_{k,i,j,l} = \frac{\omega_k \omega_i \omega_j \omega_l}{2(N+1)} \sum_{\pm} [\delta_{k,\pm j \pm l \pm m} - \delta_{k \pm j \pm l \pm m, \pm 2(N+1)}]. \quad (10)$$

where  $\delta_{i,j}$  is the Kronecker delta function and the sums  $\sum_{\pm}$  are over all combination of plus and minus signs in the equation.

The energy  $E_k$  of the  $k$ -th mode is

$$E_k = \frac{1}{2} (P_k^2 + \omega_k^2 Q_k^2) \quad (11)$$

This definition is only exact for the harmonic lattice, but serves as a good approximation for small nonlinearity, since any contributions to the energy coming from coupled modes have a pre-factor of the nonlinear strength ( $\alpha$  or  $\beta$ ).

Whenever a quantity is time-averaged, we place a line over its symbol (e.g.  $\overline{E}$ ). This represents a time-average from time  $t = 0$  to  $t = T$ , i.e.

$$\overline{E}(T) = \frac{1}{T} \int_0^T E dt \quad (12)$$

## B. Numerical Methods

For integrations involving the  $\alpha$ -FPUT model and  $\beta$ -FPUT model with  $\beta < 0$ , which have been observed to be reasonably stable [17], we use the  $SABA_2C$  symplectic integration scheme described in appendix 1 of [18]. This scheme has error  $\mathcal{O}([dt]^4)$ .

For integration of the Toda lattice, we use the  $SABA_2$  scheme i.e. the same scheme but without the corrector Hamiltonian term, giving error  $\mathcal{O}([dt]^2)$ , which was determined to be sufficient for accuracy on all parameters considered.

The  $\beta$ -FPUT model with  $\beta > 0$  has been noted to exhibit exponential instabilities, related to instabilities of the modified Korteweg-de Vries (mKdV) equation soliton solutions [19], since the mKdV equation arises from the continuum limit of the  $\beta$ -FPUT model. To reduce the need for extremely small time step sizes, we implement the symplectic integrator  $SABA_2Y8\_D$  described in [20] and in Table 2 of [21], which has error  $\mathcal{O}([dt]^8)$ . In general, we use a time step  $dt = 0.1$  unless a failure of time reversal requires us to decrease  $dt$  to improve the accuracy.

### C. Spectral Entropy

We will use spectral entropy to quantify the FPUT system's distance from equipartition at a given time. Spectral entropy is similar to Shannon information entropy [22] and is defined as

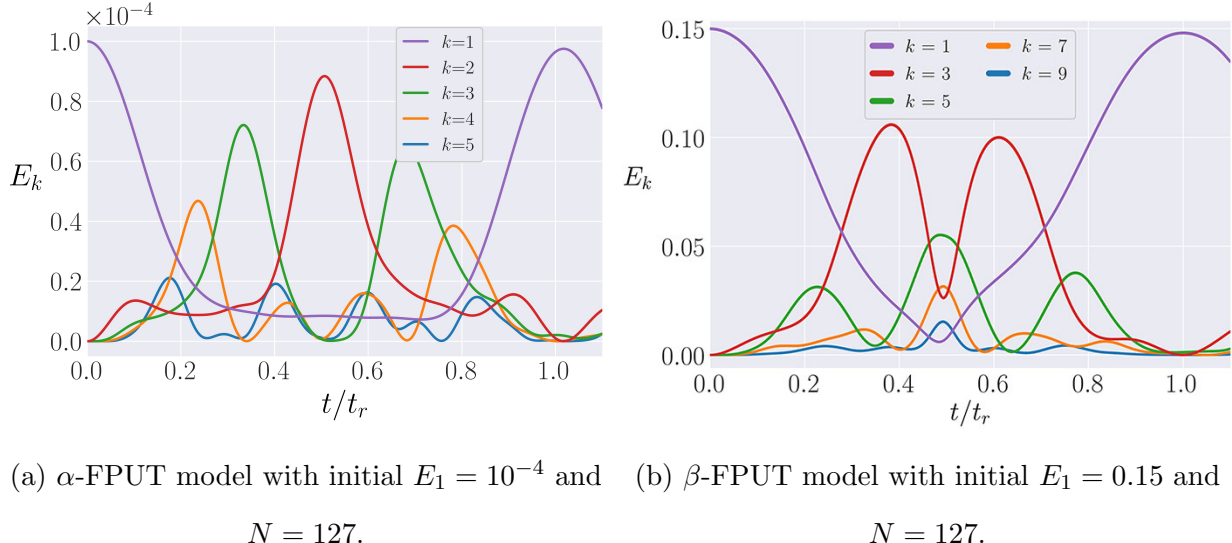
$$S(t) = - \sum_{k=1}^N e_k(t) \ln[e_k(t)] \quad (13)$$

$$e_k(t) = \frac{E_k(t)}{\sum_k E_k(t)}$$

where  $e_k(t)$  is the proportion of linear energy in mode  $k$  at time  $t$ . Spectral entropy ranges from 0 when all the energy is in one mode, to  $S_{max}$  when an equal amount of energy is present in all modes. For the  $\alpha$ -FPUT and Toda lattices, equal energy sharing corresponds to  $e_k = 1/N \forall k$ , therefore  $S_{max} = \ln(N)$ . However, the  $\beta$ -FPUT lattice remains symmetric about its center for initially symmetric excitations, and therefore energy can't spread from an even mode number to an odd, or vice versa. Due to our initial conditions which only include an odd mode, energy can only be shared among odd modes, so  $S_{max} = \ln\lceil\frac{N}{2}\rceil$ , where  $\lceil\cdot\rceil$  is the ceiling function, which rounds a number up to the next highest integer. Since this definition of spectral entropy has a different maximum value for different lattice sizes  $N$ , we can rescale it by defining the rescaled spectral entropy (henceforth entropy for short):

$$\eta(t) = \frac{S(t) - S_{max}}{S(0) - S_{max}}. \quad (14)$$

This is a convenient definition so that  $\eta$  ranges from 1 at  $t = 0$ , to 0 when energy is shared equally among all modes (equipartition), regardless of system size  $N$ .



(a)  $\alpha$ -FPUT model with initial  $E_1 = 10^{-4}$  and  $N = 127$ . (b)  $\beta$ -FPUT model with initial  $E_1 = 0.15$  and  $N = 127$ .

FIG. 1: The energy in each normal mode in the  $\alpha$ -FPUT and  $\beta$ -FPUT models as a function of time. At  $t = t_r$  the first FPUT recurrence is observed, with nearly all energy returning to its initial condition, the first normal mode. The lowest 5 allowed modes are plotted.

### III. PHENOMENA

#### A. FPUT Recurrences

One of the surprising features of the models explored by FPUT [5] was the presence of what have come to be known as “FPUT recurrences”. When all of the energy was initialized in the first normal mode, this energy was observed to diffuse to other modes quickly, but then the energy started to return back to the first normal mode, eventually nearly fully returning at what is called the recurrence time  $t_r$ . This phenomena is shown in Figure 1, which shows the energy in the lowest 5 allowed modes in the  $\alpha$ -FPUT and  $\beta$ -FPUT models as a function of time. Note that the  $\beta$ -FPUT lattice preserves symmetry about its center so with initial energy only in mode 1, only odd modes are allowed. At  $t = t_r$ , the systems have nearly recreated their initial conditions.  $t_r$  is calculated for the  $\alpha$ -FPUT model following [23] and for the  $\beta$ -FPUT model following [24]. The timescale for this recurrent behavior is many orders of magnitude shorter than the Poincaré recurrence time [25], and the recurrences continue quasi-periodically for a long time; indeed, the initial conditions considered by FPUT have yet to be driven to equipartition. However, for larger initial energy, the FPUT recurrences eventually break down, and the system is able to thermalize.

Clearly, when most of the energy is quasi-periodically returning near the initial condition, which is extremely localized, the system remains localized while these recurrences continue to happen.

FPUT recurrences have been used to study ultracold Bose gases [26], the nonlinear Schrödinger equation [27], and electron-phonon interactions [28]. Their study has extended also to higher order recurrences, such as super-recurrences [18, 29]. Their existence has been explained in various ways, most notably 1) by using  $q$ -breathers [7, 30, 31]; or 2) by the presence of solitons in the KdV (mKdV) equation, which is the continuum limit of the  $\alpha$ -FPUT ( $\beta$ -FPUT) model [6, 24, 32]. The importance of FPUT recurrences is difficult to overstate, and in this thesis we mostly explore their role in delaying the approach to equipartition.

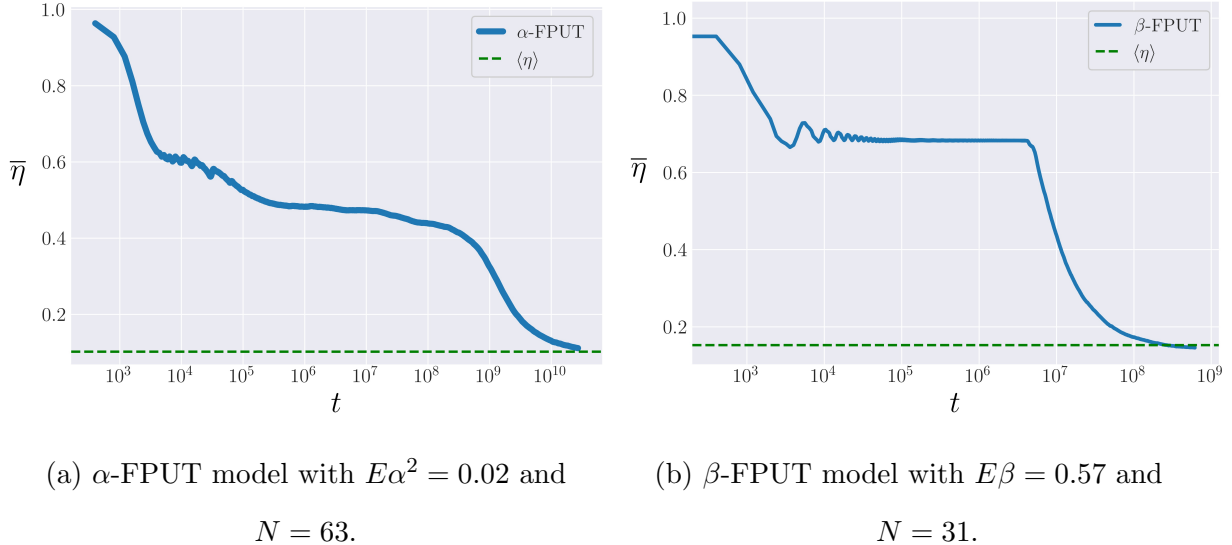


FIG. 2: The time averaged entropy as a function of time in the  $\alpha$ -FPUT and  $\beta$ -FPUT models. The ensemble average  $\langle \eta \rangle$  (from Eq. 15) is plotted and the agreement  $\bar{\eta} = \langle \eta \rangle$  appears to be stalled by a metastable state.

## B. Metastable State

The recurrence phenomenon has the effect of stalling the approach to equilibrium by keeping the system’s energy localized near its initial condition. This phenomenon has been interpreted, as early as 1982 [33], as the system having 2 time “regions”: in the first the system relaxes into an intermediate quasi-stationary state, which persists for some time, before it again relaxes, this time into its true equilibrium state defined by equipartition, such that  $\bar{\eta} = \langle \eta \rangle$ . The intermediate or “metastable” state has been studied extensively more recently by Giancarlo Benettin [13, 34–36]. His work frames the phenomena as a cross-over between predominantly integrable dynamics to the true non-integrable dynamics of the FPUT models.

First, we must note that the system is considered to be in equilibrium when  $\bar{\eta} = \langle \eta \rangle$ , where we calculate  $\langle \eta \rangle$  following Danieli [37]:

$$\langle \eta \rangle = \frac{1 - \gamma}{S_{max} - S(0)} \quad (15)$$

where  $\gamma \simeq 0.577$  is the Euler-Mascheroni constant. We are interested in the time that the metastable state lasts, before its ultimate destruction, and the system’s approach to

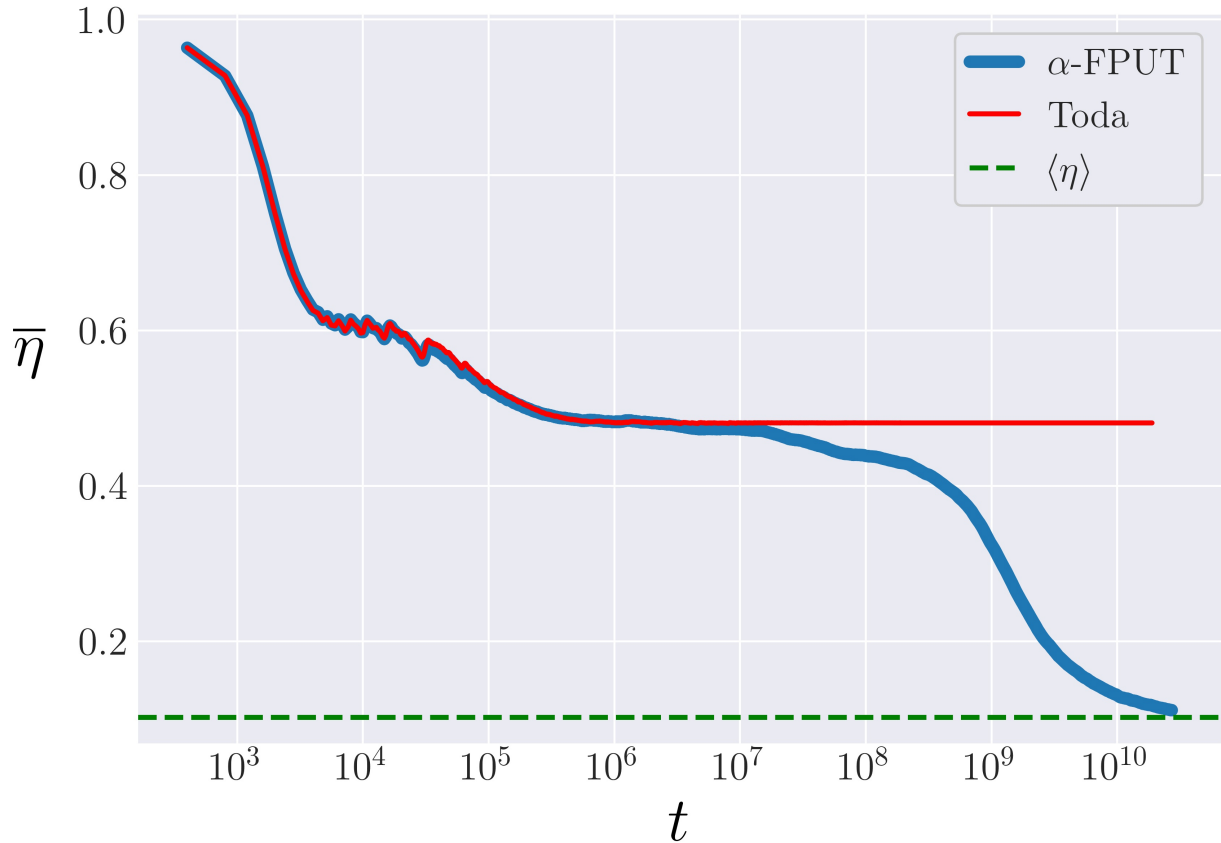


FIG. 3: The time averaged entropy  $\bar{\eta}$  as a function of time (note logarithmic scale) for both the Toda model (red) and  $\alpha$ -FPUT model (blue). Both have initial energy  $E\alpha^2 = 0.02$  and system size  $N = 63$ .

equilibrium. We call this time  $t_m$  to indicate it as the lifetime of the metastable state. In Figure 2, we visualize the metastable state in the  $\alpha$ -FPUT and  $\beta$ -FPUT models. We can see that both are qualitatively very different. While the  $\alpha$ -FPUT model appears to be decreasing in  $\bar{\eta}$  gradually, the  $\beta$ -FPUT model exhibits a distinguished plateau for a long time in the metastable state, before some mechanism causes this quasi-stationary state to collapse fairly suddenly. The features of the metastable state in the  $\alpha$ -FPUT model at first glance make it difficult to define where the metastable state ends and the approach to equilibrium begins, but we will show that this distinction is actually possible to identify when one considers the crossover time  $t_m$  to be that time at which the non-integrable behavior starts to dominate what was initially a system behaving as nearly integrable.

Up to  $\mathcal{O}(r^4)$ , the  $\alpha$ -FPUT potential (Eq. 2) can be thought of as a truncation of the

Toda potential (Eq. 4), through a convenient change of parameters. By setting  $V_0 = \lambda^{-2}$  and  $\lambda = 2\alpha$ , and Taylor expanding the Toda potential around  $r = 0$ , we get the following series expansion:

$$V_{\text{Toda}}(r) = \frac{r^2}{2} + \frac{\alpha}{3}r^3 + \frac{\alpha^2}{6}r^4 + \frac{\alpha^3}{15}r^5 + \mathcal{O}(r^6) = V_\alpha(r) + \mathcal{O}(r^4) \quad (16)$$

The  $\alpha$ -FPUT model's metastable state can be analyzed by considering its behavior to be similar to the integrable Toda lattice, before breaking off and exhibiting qualities of non-integrable systems [34]. Figure 3 demonstrates the similarity of the evolution of  $\bar{\eta}$  between the Toda model and the  $\alpha$ -FPUT model up to a certain cut off in time, after which the  $\alpha$ -FPUT model approaches the expected value of  $\bar{\eta}$ : the ensemble average  $\langle \eta \rangle$ . This comparison to the Toda lattice will allow us to define  $t_m$  in the  $\alpha$ -FPUT model. Comparing Figure 3 to Figure 2a, we see that the hard to define metastable state of Figure 2a is now made clear as roughly the time when the  $\alpha$ -FPUT model deviates from the Toda model in Figure 3.

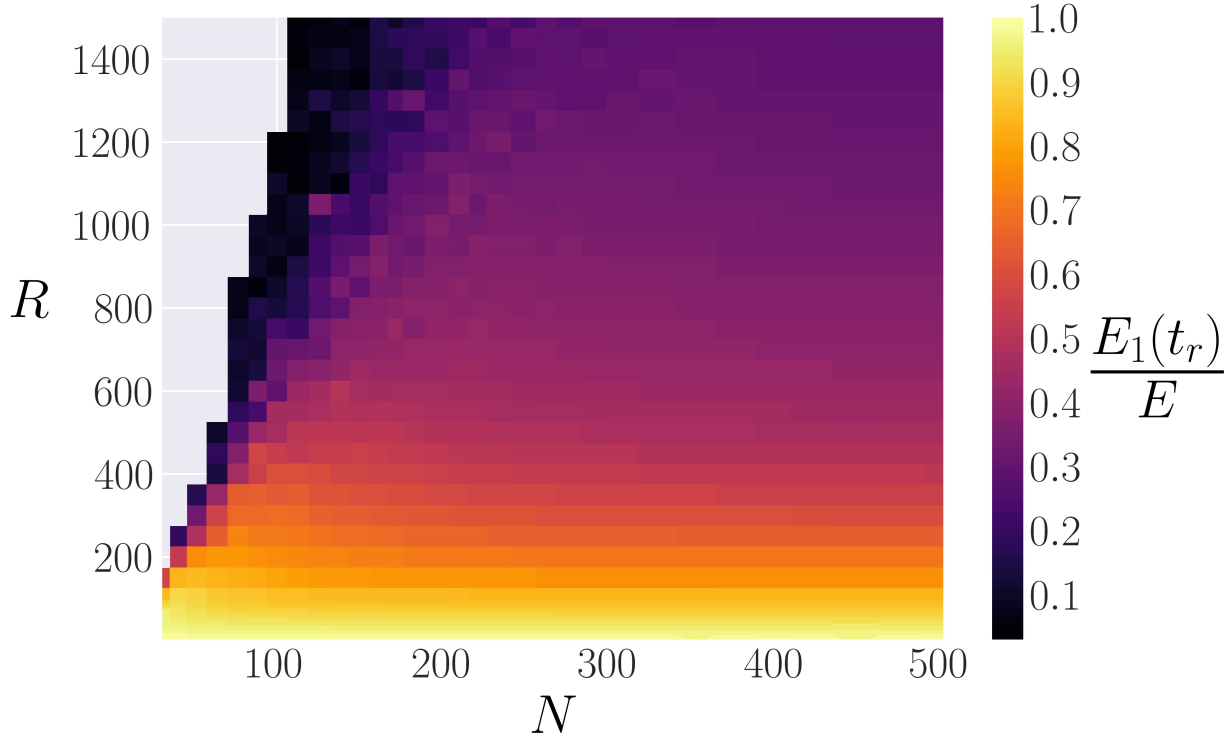


FIG. 4: Heatmap showing the “strength” of FPUT recurrences as a function of the system parameter  $R$  and system size  $N$  in the  $\alpha$ -FPUT model. Note that the gray region corresponds to initial conditions which blow up (the potential  $V(r) \rightarrow -\infty$ ) before  $1.5t_r$ .

#### IV. $\alpha$ -FPUT MODEL

##### A. Strength of FPUT Recurrences

It has been shown [23] that the time to the first FPUT recurrence ( $t_r$ ) in the  $\alpha$ -FPUT model scales as a function of an essential system parameter  $R$ , defined as:

$$R = (N + 1)^{3/2} \sqrt{E\alpha^2} \quad (17)$$

Specifically, as was shown in [23], by rescaling the FPUT recurrence time by  $(N + 1)^3$ , then for  $R \geq 10$ :

$$\frac{t_r}{(N + 1)^3} = R^{-1/2} \quad (18)$$

We use this expected value of the first FPUT recurrence time and look in the region  $0.5t_r < t < 1.5t_r$  for the maximum value of the energy in the first normal mode, and name

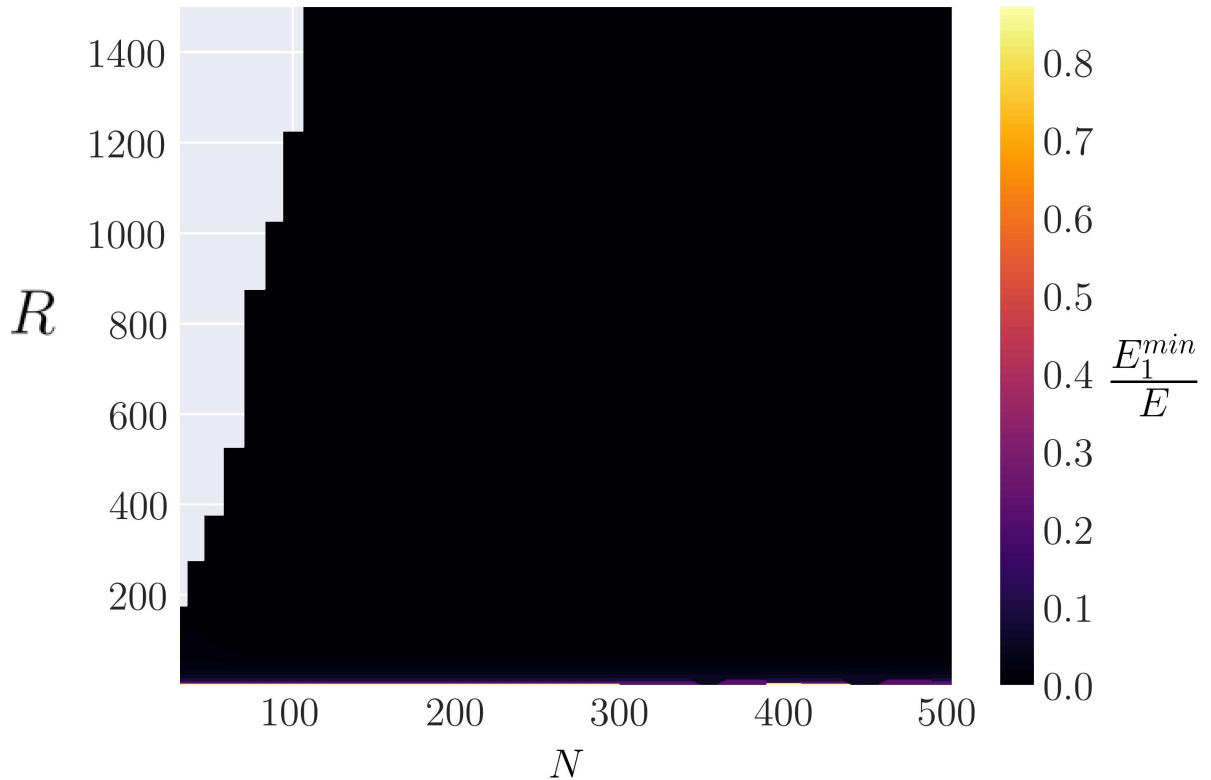


FIG. 5: The quantity  $E_1^{min}/E$ , which represents the proportion of energy that leaves the 1st normal mode before the first recurrence, is plotted as a function of system parameter  $E\alpha^2$ .

that  $E_1(t_r)$ . We can then calculate the ratio of this energy to the initial energy, and use this as a measure of the relative “strength” of the FPUT recurrence for a given value of  $R$  and  $N$ . The results are plotted in Figure 4, and demonstrate that the FPUT recurrence strength drops off as  $R$  increases - nearly independent of system size  $N$ .

This result is similar in motivation to that from Section 7 of [24], where a similar analysis was performed for the  $\beta$ -FPUT model. However, the implications are quite different: for the  $\beta$ -FPUT model, FPUT recurrences lose strength as a function of the parameter  $E\beta$  independent of  $N$  - **NOT** the essential system parameter  $S = E\beta(N + 1)$  which FPUT recurrence time scales with. For the  $\alpha$ -FPUT model, the strength of FPUT recurrences scales with  $R$ , independent of  $N$ , instead of the corresponding energy parameter  $E\alpha^2$ . It is also worth noting that while in [24] we had to define a parameter called “shareable energy” to compare the quality of FPUT recurrences between the cases  $\beta > 0$  and  $\beta < 0$ . Figure 5

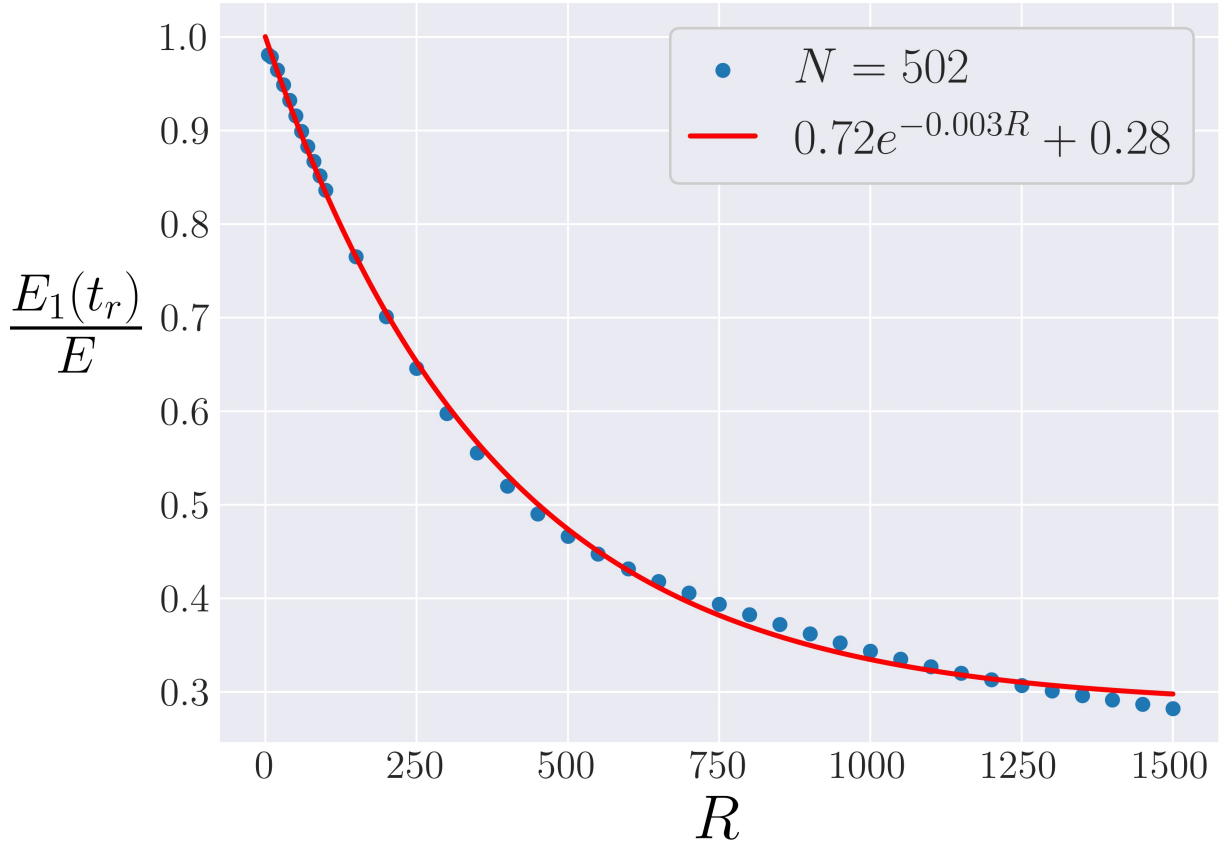


FIG. 6: The “strength” of recurrences in the  $\alpha$ -FPUT model,  $E_1(t_r)/E$  as a function of system parameter  $R$  at fixed  $N = 502$ . An exponential fit is added.

shows that this is not necessary for the  $\alpha$ -FPUT model. This figure plots the quantity:

$$\frac{E_1^{\min}}{E} \equiv \min_{0 < t < t_r} \frac{E_1(t)}{E} \quad (19)$$

which quantifies how much energy leaves the first normal mode (the initial condition), before most of it comes back at the recurrence time. Figure 5 demonstrates that for the  $\alpha$ -FPUT model, nearly all of the energy consistently leaves the first normal mode before coming back for a recurrence. This appears to be true for all  $R$  and  $N$  except in the harmonic limit ( $E\alpha^2 \rightarrow 0$ ). However, this sharing of energy is not the case for the  $\beta$ -FPUT model with  $\beta < 0$ , where roughly 70% of the energy remains in the first normal mode before a recurrence [24].

Since Figure 4 seems to show that the strength of recurrences falls off as a function of  $R$ , independent of  $N$  outside of regimes where blow-up is likely, it helps to look at systems with

the same  $N$  and plot the recurrence strength  $E_1(t_r)/E$  as a function of system parameter  $R$ . This is performed in Figure 6, and a nearly exponential decay is found. This is again in contrast to the  $\beta$ -FPUT model, where recurrence strength appears to be roughly consistent until a cut-off energy  $E\beta$  where the recurrence strength falls precipitously [24].

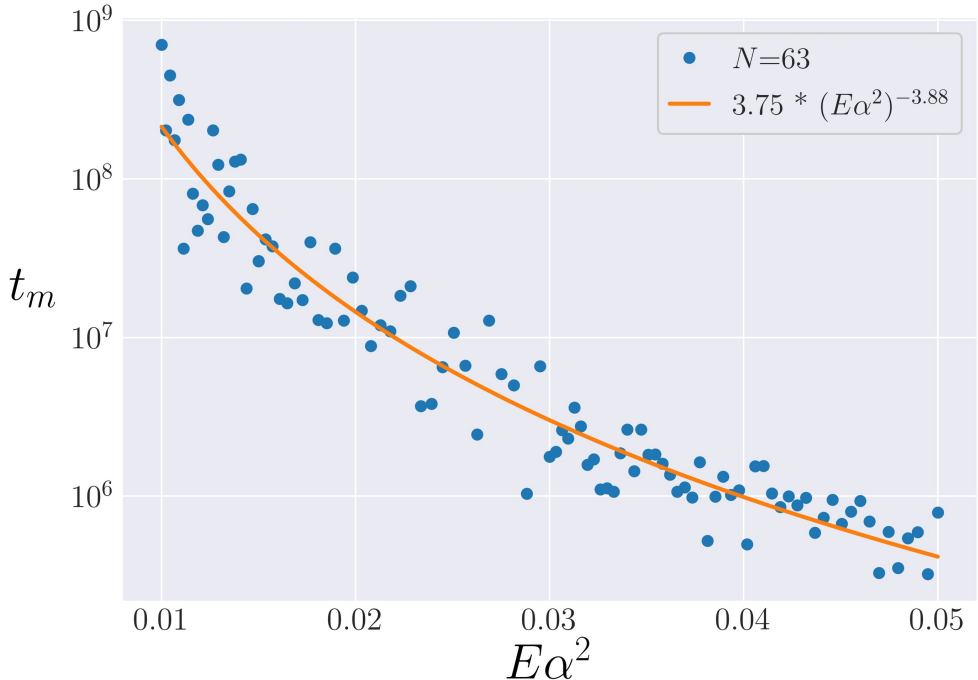


FIG. 7: An attempt at defining  $t_m$  in the  $\alpha$ -FPUT model for  $N = 63$  by defining an arbitrary tolerance and waiting for deviation from the Toda model beyond this tolerance. A power law best fit is added. Note the logarithmic scaling on the  $t_m$  axis.

## B. Lifetime of Metastable State

### 1. Procedure

We endeavor to find a scaling for the lifetime of the metastable state, through a direct comparison to the Toda model as motivated by Section III B. The most natural approach is to define some arbitrary tolerance, and look for the last time which the  $\alpha$ -FPUT model's entropy was within that tolerance of the entropy of the Toda model. Doing so, however, reveals a key feature of the metastable state. The results of following this procedure for  $N = 63$  are shown in Figure 7. Even though a clear power law scaling emerges, the data is quite noisy around this scaling. This noisiness appears to be an inherent feature of the chaotic nature of the  $\alpha$ -FPUT model around the metastable state.

Note that since the Toda model is integrable, its dynamics can in theory be broken down into actions that remain constant in time and angles that evolve periodically in time. The picture of the metastable state of the  $\alpha$ -FPUT model presented by Benettin et al. in [36]

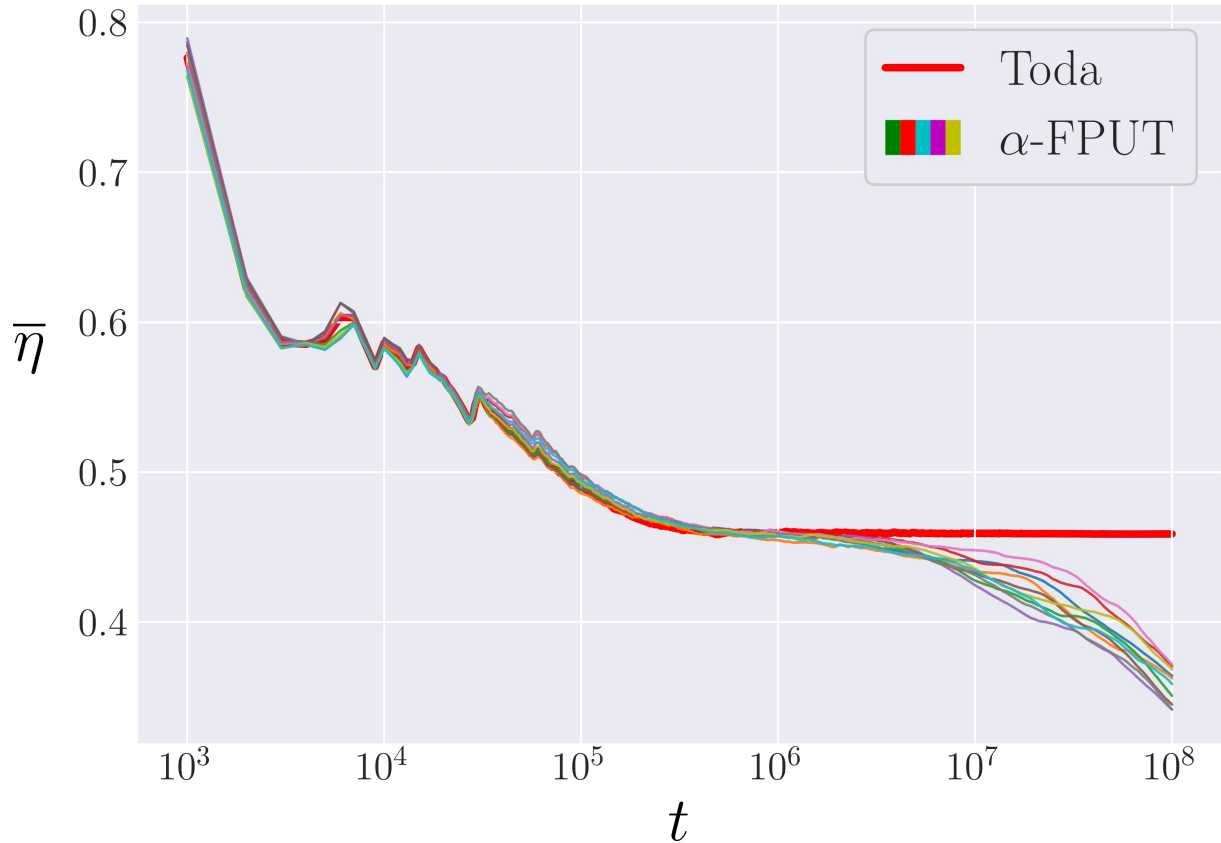


FIG. 8: The time-averaged entropy in the Toda model (red curve) compared to 10 bins of  $\alpha$ -FPUT trajectories, each made up of the average of 10 random phases. All systems are fixed at energy  $E\alpha^2 = 0.028$  and system size  $N = 63$ .

is that there are two time scales in the system. In the first one the actions of the Toda model remain nearly constant even in the  $\alpha$ -FPUT model, while the Toda angles evolve on tori, leading to a behavior very similar to that of the Toda model. Eventually, on a longer time scale, the Toda actions start to diffuse throughout the phase space, eventually leading to ergodicity and equipartition. The short time scale where the Toda actions remain nearly constant is the metastable state currently under scrutiny. An important aspect of the transition to diffusing actions is that this diffusion behaves chaotically, with finite maximal Lyapunov exponents as described in [36]. This leads to an exponential sensitivity to initial conditions for when the diffusion of action variables dominates the dynamics, which explains the noise in Figure 7. To quantify the effect of initial conditions, we conduct bin averaging over initial conditions.

Note that from Equation 11, the energy initially given to the first normal mode can be distributed either in canonical position or momentum. We define the “phase”  $\theta$  between our canonical coordinates as:

$$\theta = \tan^{-1} \left( \frac{P_1(t)}{\omega_1 Q_1(t)} \right) \quad (20)$$

We can then initialize systems with the same condition  $E_1(0) = E$ , i.e. the same point in energy space, but slightly separated in phase space by distributing along the oval of canonical coordinates defined by rotating  $\theta$ . In the following, we take 100 random phases for every choice of energy and bin them together to create 10 bins which are each the average of 10 trials with different phases. An example of the results is shown in Figure 8, where each  $\alpha$ -FPUT curve represents an average over 10 random phases. Figure 8 demonstrates that each of the  $\alpha$ -FPUT trials remains close to the Toda model, up until some time where the entropy starts to decrease below the Toda model entropy (red curve), and then the  $\alpha$ -FPUT trajectories start to diverge, not only from the Toda trajectory but also from each other.

We gain two advantages from binning in this manner: 1) we now have a natural length to use as a tolerance cut-off to define separation between  $\alpha$ -FPUT model and Toda model that isn’t arbitrary: the standard deviation of each bin; 2) averaging over 10 different bins again gives us an error bar on our measurement of  $t_m$  for a given energy. Our procedure is now as follows: take 10 trials for the  $\alpha$ -FPUT model with random phases and average their entropy together. Find the last time that the Toda model’s entropy was within 1 standard deviation of this bin average. Repeat this for 10 total bins, and average those times together to get a measurement of  $t_m$  with an error bar.

Performing this operation reveals a surprising result, shown in Figure 9. If we look at the bin standard deviation ( $\sigma$ ), averaged over bins ( $\bar{\sigma}$ ), over time, there is a feature similar to a phase transition in the plot. The time at which this occurs just so happens to line up with the time  $t = t_m$  as defined in our above procedure. Since our procedure looks when  $\bar{\sigma}$  in the  $\alpha$ -FPUT model is greater than  $\sigma$  outside of  $\bar{\sigma}$  in the Toda model, this means  $\bar{\sigma}$  is falling quicker than  $\sigma$  is rising in Figure 9, which is significant. This also further validates the point of view that  $t_m$  represents a transition from mostly integrable dynamics to chaotic, non-integrable dynamics. The growth in  $\bar{\sigma}$  for  $t > t_m$  shows that initially nearby systems are deviating in time, whereas for  $t < t_m$ ,  $\bar{\sigma}$  is seen to be relatively bounded in time. This also serves to validate our procedure to measure  $t_m$ .

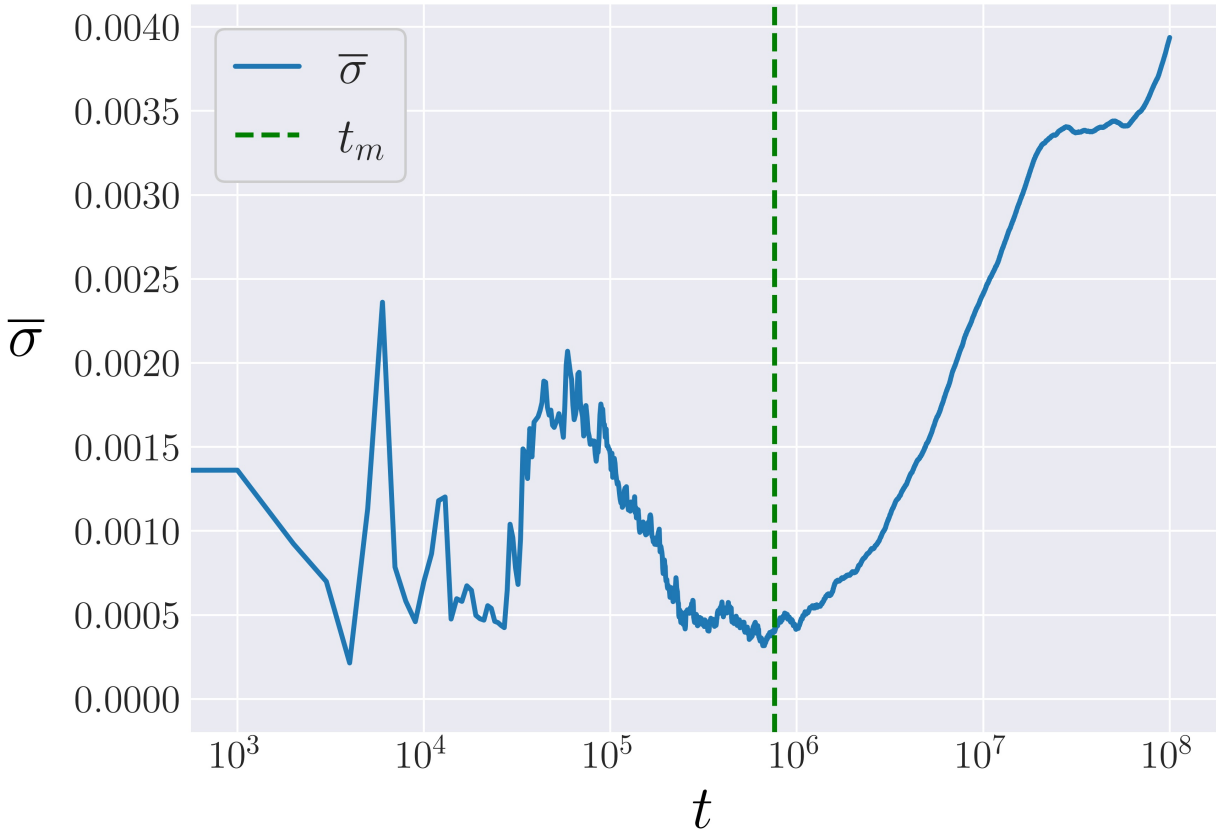


FIG. 9: The bin deviation, averaged over bins, again for  $E\alpha^2 = 0.028$  and  $N = 63$  in the  $\alpha$ -FPUT model. The measure value for  $t_m$  is marked as a vertical dashed green line.

## 2. Analysis

We apply the procedure described in the previous section and iterate across a range of energies, for  $N = 63, 127$ , and  $255$ . We determined that system size  $N = 31$  was too small and gave erratic results incompatible with the thermodynamic limit. For a discussion of small system size effects in the  $\alpha$ -FPUT model, see [38]. We choose system sizes such that  $N + 1$  is a power of 2, to avoid resonances discussed in [39].

The results are shown in Figure 10. The length of each data point is the extent of its bin error. Each system size appears to follow its own trend for high energies. Then, for low energies the data appear to overlap, *regardless of system size*. In this regime,  $t_m$  is seen to follow a power law, roughly consistent with an exponent of  $-4.9$  as shown by the red dashed line in Figure 10. A few simulations indicate that this overlap and scaling is consistent for higher system sizes too.

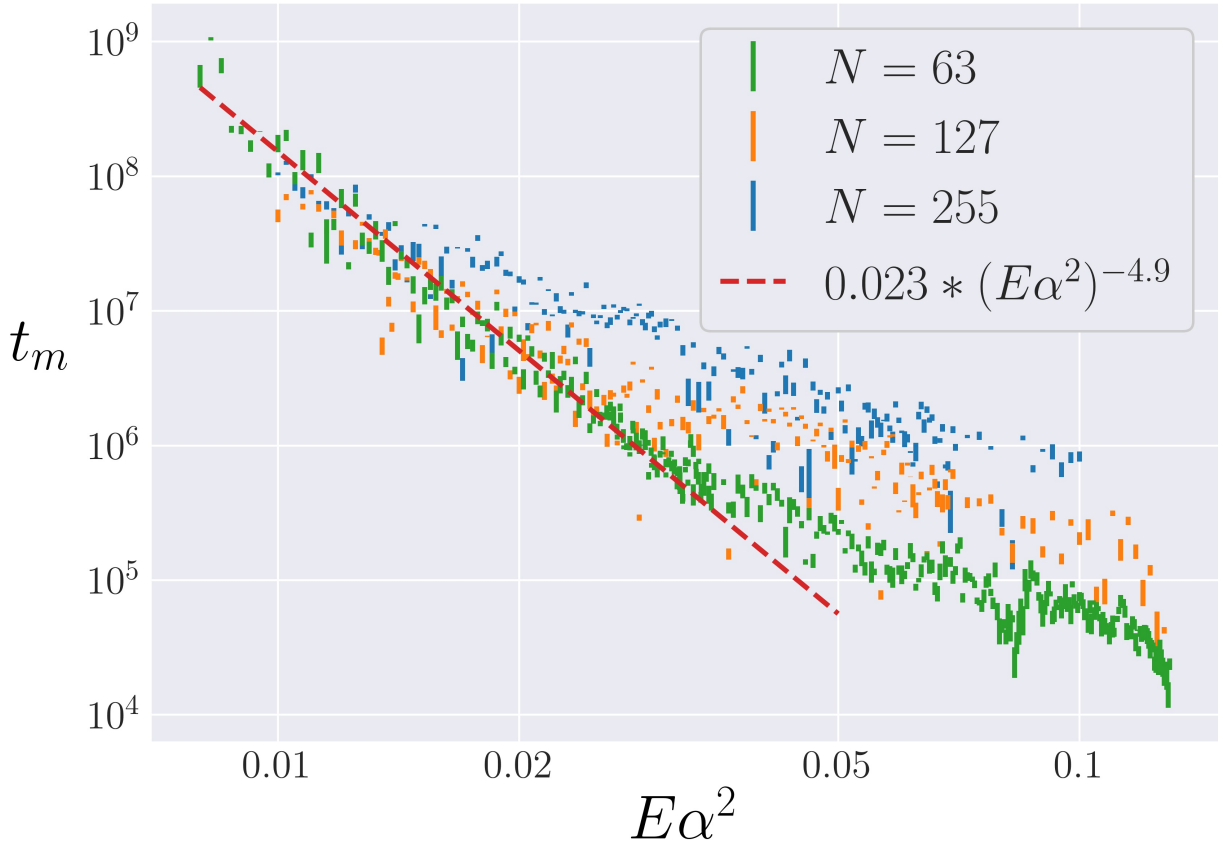


FIG. 10: The lifetime of the metastable state as a function of  $E\alpha^2$  for  $N = 63, 127$ , and  $255$ . The height of each data point represents its bin error. In the  $E\alpha^2 \rightarrow 0$  limit the data is seen to follow a power law, in dashed red. Note logarithmic scale on both axes.

One interesting aspect of Figure 10 is that the error in the noise (shown by the scattering of the data) seems to be larger than the error due to phase averaging and binning (shown by height of data points). In order to account for these two possible sources of chaotic noise, we bin data into groups of 20 consecutive energies to estimate the noise in energy. Then we assume that phase noise ( $\sigma_\theta$ ) and energy noise ( $\sigma_E$ ) are independent, and add them together as

$$\sigma = \sqrt{\sigma_\theta^2 + \sigma_E^2} \quad (21)$$

to perform error propagation and get an upper bound on the noise. The results are presented in Figure 11. This gives a better idea of the noise (inherent since the metastable state signals the onset of chaos) in the lifetime of the metastable state.

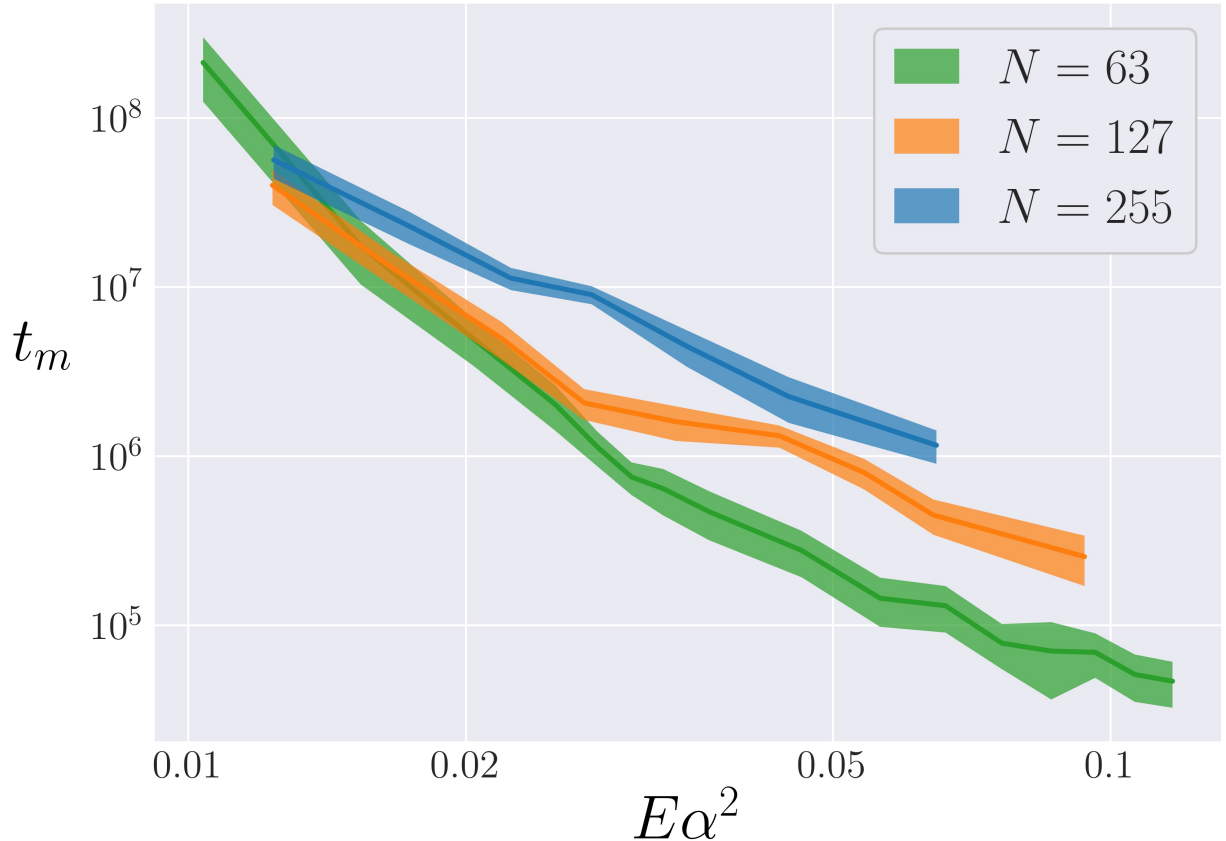


FIG. 11: Lifetime of the metastable state similar to Figure 10 except nearby energies are binned to get an upper bound on the noise as a combination of phase and energy error.

Note logarithmic scale on both axes.

One more region of interest is as  $E\alpha^2$  increases, and how  $t_m$  behaves.  $t_m$  is plotted for larger energies in Figure 12. An interesting aspect of this plot is that the error bars, both for  $\sigma_\theta$  and  $\sigma_E$ , decrease dramatically around  $E\alpha^2 = 0.145$ , where the calculated value of  $t_m$  is seen to start increasing. This region appears to correspond to the  $\alpha$ -FPUT model deviating before the beginning of the plateau shown in Figure 3, and therefore we say that metastable state stops forming for systems with energy higher than this value. The measured value of  $t_m$  follows from our procedure but just shows that the systems are deviating on a very short time scale, i.e. there is no metastable state.

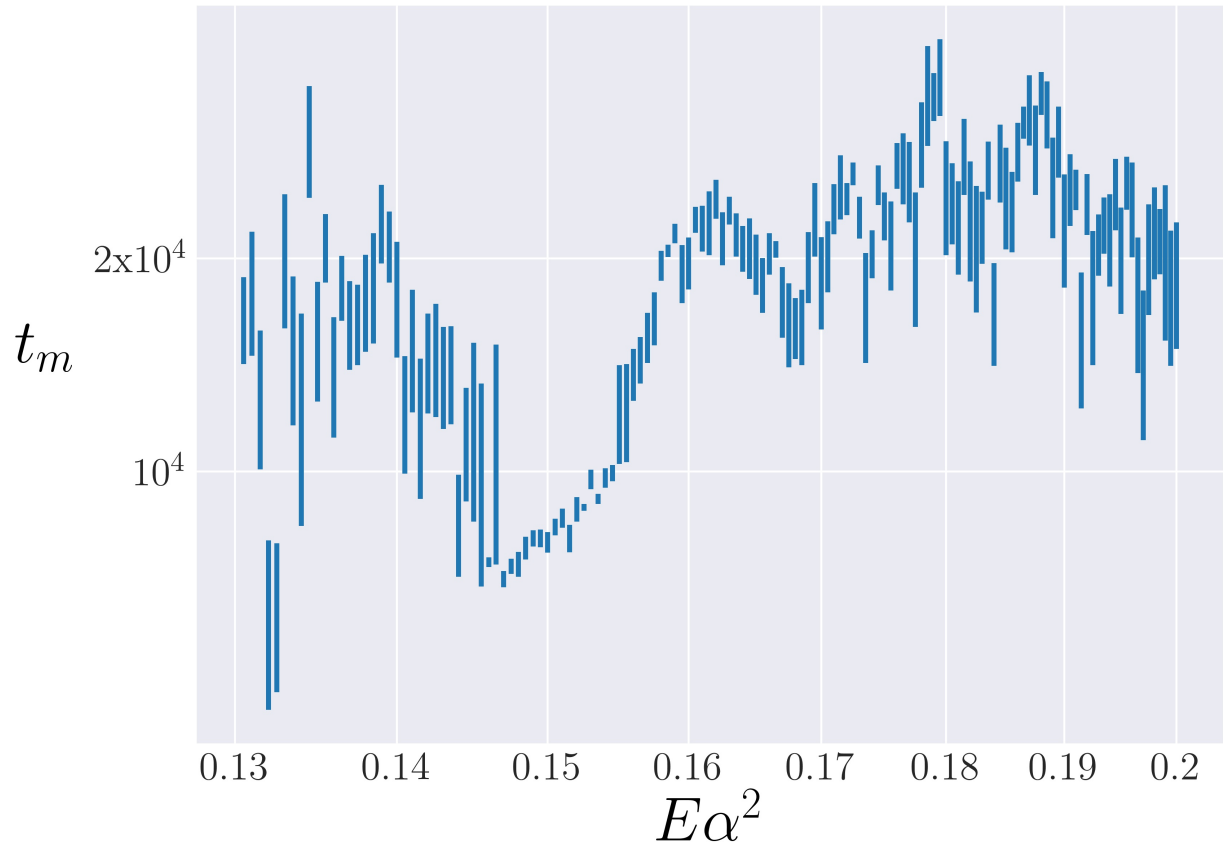


FIG. 12:  $t_m$  is plotted as a function of  $E\alpha^2$  for  $N = 63$ , for higher energies than in Figure 10. Note logarithmic scale on both axes.

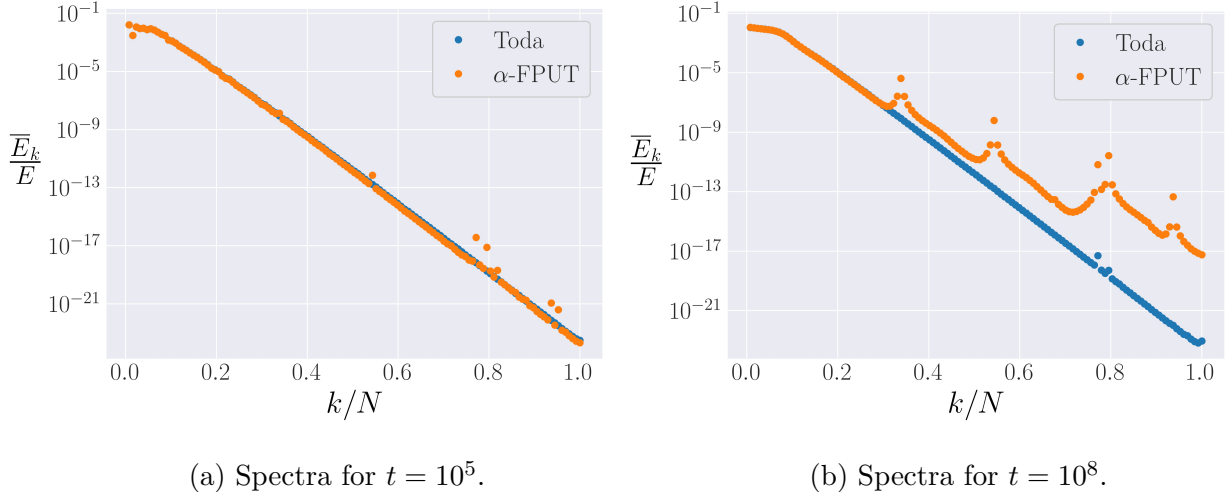


FIG. 13: The spectra of the  $\alpha$ -FPUT and Toda models for system parameter  $R = 75$  and  $N = 127$ . Spectra are compared at two different times.

### C. Spectrum

A qualitative picture of the method for the destruction of the metastable state can be seen by comparing the spectrum of the  $\alpha$ -FPUT model to that of the Toda model. By plotting the time averaged energy in each normal mode, at a given time, we have access to many more degrees of freedom than simply looking at the entropy, and we can therefore get a fuller picture. For short times, we expect that the spectrum of the  $\alpha$ -FPUT and Toda models look mostly identical. This is indeed the case. As time goes on, the Toda spectrum flattens out to an exponential tail, which is the shape of the  $\alpha$ -FPUT spectrum in the metastable state as well. However, some higher modes start to gain energy, and spread this to the modes nearby them. This process continues until most higher modes are excited and the system approaches equipartition. This behavior is demonstrated in Figure 13.

Figure 13a is plotted after  $t = 10^5$ , and shows that the spectra of the  $\alpha$ -FPUT model and the Toda model largely agree so far. Then, Figure 13b is plotted after  $t = 10^8$ , and we can see that resonances have caused local peaks in the  $\alpha$ -FPUT spectrum, which diffuse energy into the modes around them. This has the effect of lifting the spectrum at each resonance, a process which continues until the system reaches equipartition. In [40], Onorato et al. showed that four-wave resonances in the thermodynamic limit of the  $\alpha$ -FPUT model lead to irreversible energy mixing. It was also shown that six-wave interactions are always possible,

and lead to irreversible energy mixing. It is possible that the two largest peaks in the spectra of the  $\alpha$ -FPUT model (Figure 13b) are actually made of two resonant modes each, so it is unclear if this is an example of a four-wave or six-wave resonance. Another peculiarity in Figure 13b are the apparent high-k modes in the Toda model which lie well above an exponential tail, even after a long time. The peaks around  $k/N \simeq 0.8$  do not appear to be a numerical artifact, so there could possibly be resonances in the integrable limit (which do *not* lead to irreversible energy mixing).

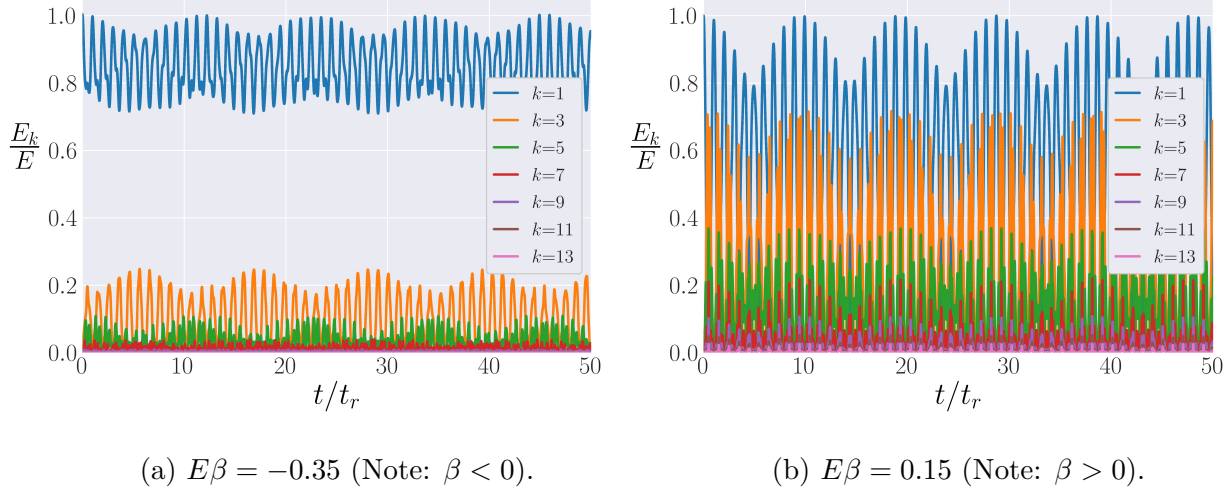


FIG. 14: The energy in the lowest 13 modes as a function of time for  $N = 127$ , and the two choices of the sign of  $\beta$ , in the  $\beta$ -FPUT model. Energy in each mode is rescaled by initial energy  $E$  and time is rescaled by the FPUT recurrence time  $t_r$ .

## V. $\beta$ -FPUT MODEL

### A. Comparison Between $\beta > 0$ and $\beta < 0$

A surprising difference between the FPUT recurrences in the  $\beta$ -FPUT model for the different signs of  $\beta$  was noted in Section 7 of [24]. The difference is qualitatively demonstrated in Figures 14a ( $\beta < 0$ ) and 14b ( $\beta > 0$ ), which show the proportion of total energy in each of the first 13 modes against time. Results are plotted for the first 50 FPUT recurrences, with the FPUT recurrence time  $t_r$  calculated using the results from [24]. For a system with  $\beta > 0$ , the energy almost entirely leaves the first normal mode before coming back at an FPUT recurrence (as demonstrated by Figure 1, which is essentially a zoom into Figure 14b). When  $\beta < 0$ , nearly 70% of the energy always remains in the first normal mode during the metastable state.

When the distribution of energy among all normal modes (energy spectrum) in the metastable state is considered, however, the two systems are relatively similar. Figures 15a ( $\beta < 0$ ) and 15b ( $\beta > 0$ ) plot the spectrum of the  $\beta$ -FPUT system, i.e. the time averaged energy in each mode. The time averages are computed after 50 FPUT recurrences have occurred. Both spectra follow an exponential decay, with a few peaks in the spectra raising further questions. In [40], Onorato et al. showed that six-wave resonances lead to ir-

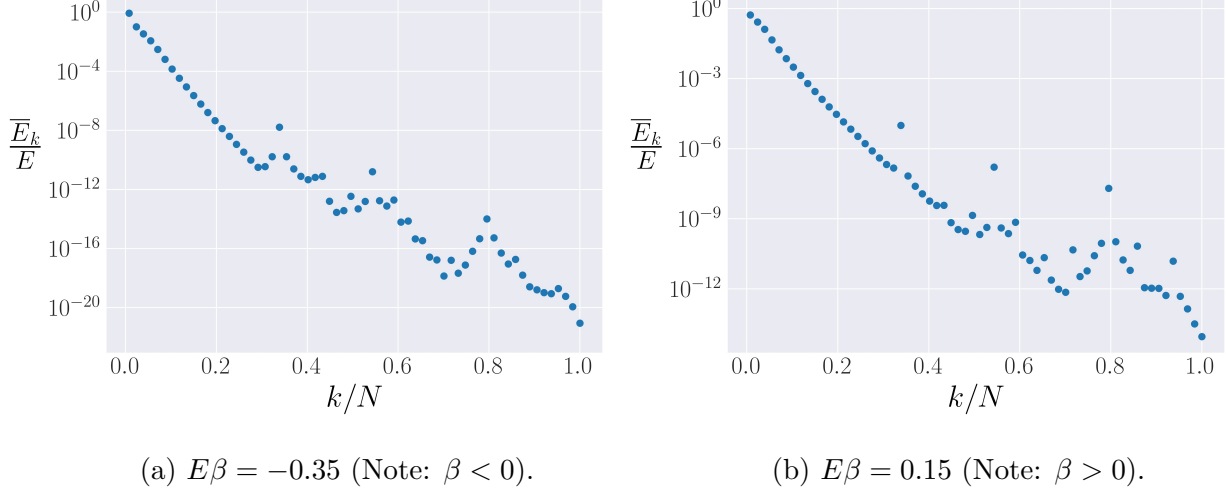


FIG. 15: Time averaged energies in each mode for  $N = 127$ , as a function of mode number  $k$ . The average is taken after 50 FPUT recurrences have taken place.

reversible energy mixing, these peaks might correspond to those resonances. This possibility is under further investigation.

Figure 15 shows that the differences noted in Figure 14 is only evident between the 1st and 3rd normal modes, all other modes follow a qualitatively similar distribution. It is possible that for  $\beta < 0$ , the  $k = 1$  mode engages in the energy diffusing resonance while  $k = 1$  is not a resonant mode for  $\beta > 0$ . This would explain the lack of energy mixing for  $\beta < 0$  and the local peak at  $k = 1$  in the spectrum (Figure 15a).

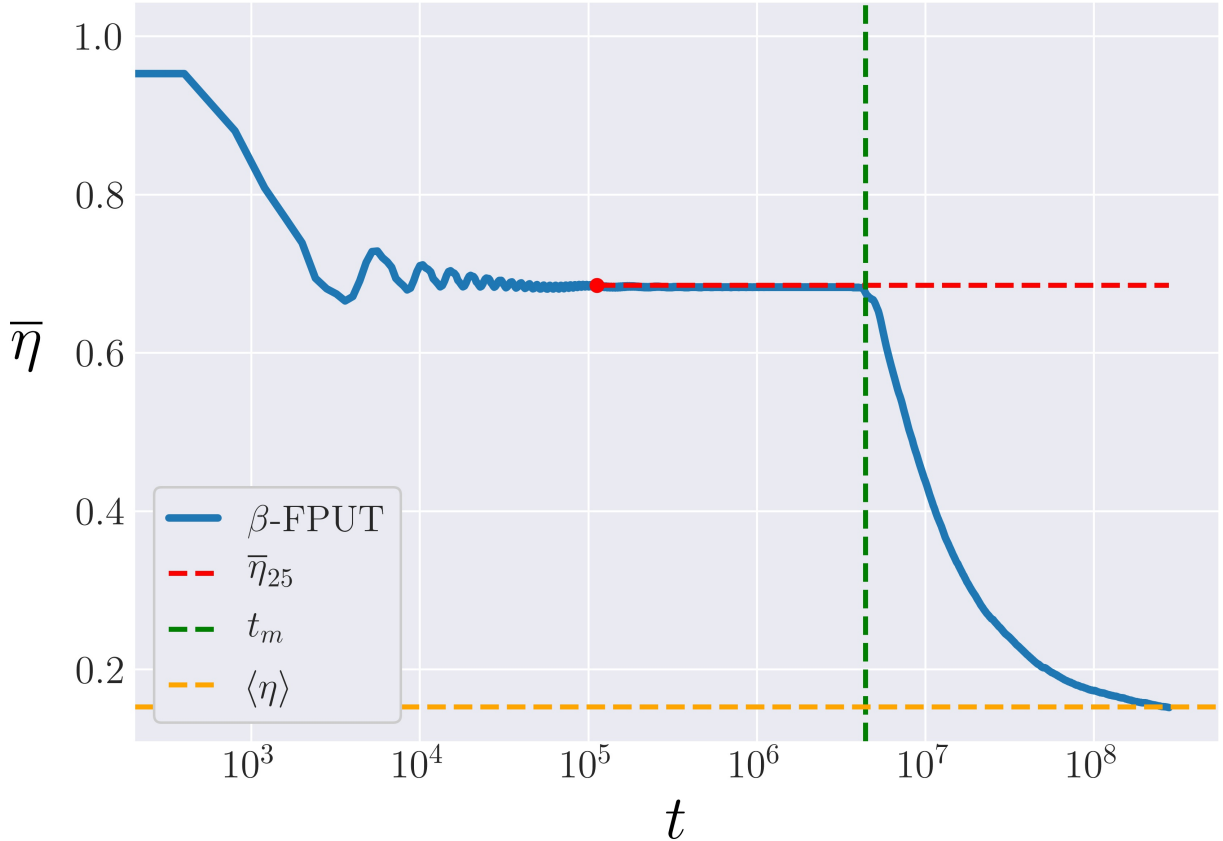


FIG. 16: The entropy of the  $\beta$ -FPUT system for  $N = 31$ ,  $E\beta = 0.57$ . The calculated value of  $\bar{\eta}$  in the metastable state,  $\bar{\eta}_{25}$ , is shown starting at the time of the 25th recurrence as a red dashed line, and the calculated metastable lifetime,  $t_m$ , shown as a vertical green line.

The ensemble average,  $\langle \eta \rangle$ , is shown in orange.

## B. Lifetime of Metastable State

As depicted in Figure 2b, the metastable state in the  $\beta$ -FPUT model ends much more abruptly than that of the  $\alpha$ -FPUT model. However, no integrable lattice model exists for which the  $\beta$ -FPUT potential is a truncation. Instead, the  $\beta$ -FPUT model is most closely a perturbation of the harmonic lattice. We will endeavor to nonetheless describe a procedure for calculating  $t_m$  in the  $\beta$ -FPUT model, an exhaustive calculation of which is outside the computational scope of this project due to the added computational cost of using an integration scheme accurate enough to ensure that the collapse of the metastable state is not a numerical artifact (see Section II B).

As in the  $\alpha$ -FPUT model, we run 100 trials with random initial phases, and bin them into

10 bins with 10 trials each. First, we define  $\bar{\eta}_{25}$ , the time averaged entropy after 25 FPUT recurrence times, averaged across the 10 trials in a bin. The recurrence time is calculated following [24]. The number 25 was chosen because this allows the system to relax into its metastable state. Then,  $\bar{\eta}$  tends to be nearly constant in time up until a critical time where it starts relaxing to equilibrium. We can find this critical time,  $t_m$ , by calculating a deviation of  $\bar{\eta}$  from  $\bar{\eta}_{25}$  by more than the bin standard deviation of the 10 trials. Then, averaging this result over the 10 bins gives a measurement of  $t_m$  with error bars.

## VI. CONCLUSION

In this thesis we have performed a broad analysis of the metastable state in the  $\alpha$ -FPUT and  $\beta$ -FPUT models, both quantitative and qualitative. We started with a visualization of the metastable using spectral entropy ( $\eta$ ). This single degree of freedom has the power to quantify the distance to equipartition. A description of this manner allowed us to follow G. Benettin [34] in viewing the  $\alpha$ -FPUT model as a truncation of the integrable Toda model.

We first visualized the strength of recurrences in the  $\alpha$ -FPUT model, following the results from S. Pace [24] on the  $\beta$ -FPUT model. This yielded the surprising result that the recurrence strength is a function only of the essential system parameter  $R = (N + 1)^{3/2} \sqrt{E\alpha^2}$  in the  $\alpha$ -FPUT model – whereas the strength of recurrences in the  $\beta$ -FPUT model scale with the energy  $E\beta$  and not the essential system parameters  $S = E\beta(N + 1)$ . The strength of recurrences was shown to decay exponentially with  $R$ , independent of system size  $N$ .

Next, we devised a method to measure the lifetime of the metastable state  $t_m$  in the  $\alpha$ -FPUT model. Our procedure involved averaging over random initial phases in the  $P_1$ - $Q_1$  plane (at fixed energy  $E_1 = \frac{1}{2}(P_1^2 + \omega_k^2 Q_1^2)$ ). This bin average provided a relevant length distance, the standard deviation, from which we could determine when the  $\alpha$ -FPUT model trajectories break off from the entropy of the Toda model. Applying this procedure yielded Figure 10, which shows  $t_m$  as a function of  $E\alpha^2$  for different  $N$ . Surprisingly, as  $E\alpha^2 \rightarrow 0$ , the data for different  $N$  collapses onto the same power law with exponent  $-4.9$ .

We explored the spectrum of the  $\alpha$ -FPUT model, compared to that of the Toda model. This analysis suggestively demonstrated a method for an irreversible energy dissipation process proven by Onorato et al. [40]: four-wave and six-wave resonances. These preliminary results appear to confirm the presence of these resonances, but more work is needed on the subject.

Finally, we turned our attention to the  $\beta$ -FPUT model. We explored the two different signs of  $\beta$ , something which is not interesting in the  $\alpha$ -FPUT model since the  $\alpha$ -FPUT Hamiltonian is symmetric under  $\alpha \rightarrow -\alpha$ . The spectra for the  $\beta$ -FPUT model suggestively point to resonances leading to equipartition as well. Last, a procedure is described for calculating  $t_m$  in the  $\beta$ -FPUT model, a very different task than for the  $\alpha$ -FPUT model since the  $\beta$ -FPUT model is not the truncation of an integrable model.

- 
- [1] R. K. Pathria and P. D. Beale, *Statistical Mechanics*. Elsevier, third ed., 2011.
  - [2] J. J. Waterson, “On the Physics of media that are composed of free and perfectly elastic molecules in a state of motion,” *Royal Society*, vol. 5, Jan. 1851.
  - [3] S. T. Thornton and A. F. Rex, *Modern physics for scientists and engineers*. Boston, MA: Cengage Learning, 4th ed ed., 2013.
  - [4] J. Wang, G. Casati, and G. Benenti, “Classical Physics and Blackbody Radiation,” *Physical Review Letters*, vol. 128, p. 134101, Mar. 2022.
  - [5] E. Fermi, J. R. Pasta, S. Ulam, and M. Tsingou, “Studies of Nonlinear Problems, I,” *Los Alamos Report*, no. LA-1940, 1955.
  - [6] N. J. Zabusky and M. D. Kruskal, “Interaction of ”Solitons” in a Collisionless Plasma and the Recurrence of Initial States,” *Physical Review Letters*, vol. 15, pp. 240–243, Aug. 1965.
  - [7] S. Flach, M. V. Ivanchenko, and O. I. Kanakov, “ $q$ -Breathers and the Fermi-Pasta-Ulam Problem,” *Physical Review Letters*, vol. 95, p. 064102, Aug. 2005.
  - [8] D. K. Campbell, P. Rosenau, and G. M. Zaslavsky, “Introduction: The Fermi–Pasta–Ulam problem—The first fifty years,” *Chaos: An Interdisciplinary Journal of Nonlinear Science*, vol. 15, p. 015101, Mar. 2005.
  - [9] G. Gallavotti, ed., *The Fermi-Pasta-Ulam problem: a status report*. No. 728 in Lecture notes in physics, Berlin ; New York: Springer, 2008.
  - [10] G. P. Berman and F. M. Izrailev, “The Fermi–Pasta–Ulam problem: Fifty years of progress,” *Chaos: An Interdisciplinary Journal of Nonlinear Science*, vol. 15, p. 015104, Mar. 2005.
  - [11] M. Porter, N. Zabusky, B. Hu, and D. Campbell, “Fermi, Pasta, Ulam and the Birth of Experimental Mathematics,” *American Scientist*, vol. 97, no. 3, p. 214, 2009.
  - [12] T. P. Weissert, *The genesis of simulation in dynamics: pursuing the Fermi-Pasta-Ulam problem*. New York: Springer, 1997.
  - [13] G. Benettin, A. Carati, L. Galgani, and A. Giorgilli, “The Fermi—Pasta—Ulam Problem and the Metastability Perspective,” in *The Fermi-Pasta-Ulam Problem* (G. Gallavotti, ed.), vol. 728, pp. 151–189, Berlin, Heidelberg: Springer Berlin Heidelberg, 2008. Series Title: Lecture Notes in Physics.
  - [14] M. Toda, “Studies of a non-linear lattice,” *Physics Reports*, vol. 18, pp. 1–123, May 1975.

- [15] D. Sholl, “Modal coupling in one-dimensional anharmonic lattices,” *Physics Letters A*, vol. 149, pp. 253–257, Oct. 1990.
- [16] R. Bivins, N. Metropolis, and J. R. Pasta, “Nonlinear coupled oscillators: Modal equation approach,” *Journal of Computational Physics*, vol. 12, pp. 65–87, May 1973.
- [17] C. F. Driscoll and T. M. O’Neil, “Explanation of Instabilities Observed on a Fermi-Pasta-Ulam Lattice,” *Physical Review Letters*, vol. 37, pp. 69–72, July 1976.
- [18] S. D. Pace and D. K. Campbell, “Behavior and breakdown of higher-order Fermi-Pasta-Ulam-Tsingou recurrences,” *Chaos: An Interdisciplinary Journal of Nonlinear Science*, vol. 29, p. 023132, Feb. 2019.
- [19] C. Driscoll and T. O’Neil, “Those ubiquitous, but oft unstable, lattice solitons,” *Rocky Mountain Journal of Mathematics*, vol. 8, Mar. 1978.
- [20] C. Danieli, B. Many Manda, T. Mithun, and C. Skokos, “Computational efficiency of numerical integration methods for the tangent dynamics of many-body Hamiltonian systems in one and two spatial dimensions,” *Mathematics in Engineering*, vol. 1, no. 3, pp. 447–488, 2019.
- [21] H. Yoshida, “Construction of higher order symplectic integrators,” *Physics Letters A*, vol. 150, pp. 262–268, Nov. 1990.
- [22] C. E. Shannon, “A Mathematical Theory of Communication,” *The Bell System Technical Journal*, vol. XXVII, p. 45, July 1948.
- [23] C. Lin, C. Goedde, and S. Lichter, “Scaling of the recurrence time in the cubic Fermi-Pasta-Ulam lattice,” *Physics Letters A*, vol. 229, pp. 367–374, June 1997.
- [24] S. D. Pace, K. A. Reiss, and D. K. Campbell, “The  $\beta$  Fermi-Pasta-Ulam-Tsingou recurrence problem,” *Chaos: An Interdisciplinary Journal of Nonlinear Science*, vol. 29, p. 113107, Nov. 2019.
- [25] L. Barreira, “Poincaré recurrence: old and new,” in *XIVth International Congress on Mathematical Physics*, (Lisbon, Portugal), pp. 415–422, World Scientific, Mar. 2006.
- [26] I. Danshita, R. Hipolito, V. Oganesyan, and A. Polkovnikov, “Quantum damping of Fermi-Pasta-Ulam revivals in ultracold Bose gases,” *Progress of Theoretical and Experimental Physics*, vol. 2014, pp. 43I03–0, Apr. 2014.
- [27] E. Infeld, “Quantitive Theory of the Fermi-Pasta-Ulam Recurrence in the Nonlinear Schrödinger Equation,” *Physical Review Letters*, vol. 47, pp. 717–718, Sept. 1981.
- [28] G. Kopidakis, C. M. Soukoulis, and E. N. Economou, “Electron-phonon interactions and

- recurrence phenomena in one-dimensional systems,” *Physical Review B*, vol. 49, pp. 7036–7039, Mar. 1994.
- [29] G. Drago and S. Ridella, “Some more observations on the superperiod of the non-linear FPU system,” *Physics Letters A*, vol. 122, pp. 407–412, June 1987.
- [30] S. Flach, M. V. Ivanchenko, and O. I. Kanakov, “ $q$ -breathers in Fermi-Pasta-Ulam chains: Existence, localization, and stability,” *Physical Review E*, vol. 73, p. 036618, Mar. 2006.
- [31] H. Christodoulidi, C. Efthymiopoulos, and T. Bountis, “Energy localization on  $q$ -tori, long-term stability, and the interpretation of Fermi-Pasta-Ulam recurrences,” *Physical Review E*, vol. 81, p. 016210, Jan. 2010.
- [32] J. Zabusky, “Nonlinear Lattice Dynamics and Energy Sharing,” *Journal of the Physical Society of Japan*, vol. 26, p. 7, 1969.
- [33] F. Fucito, F. Marchesoni, E. Marinari, G. Parisi, L. Peliti, S. Ruffo, and A. Vulpiani, “Approach to equilibrium in a chain of nonlinear oscillators,” *Journal de Physique*, vol. 43, no. 5, pp. 707–713, 1982.
- [34] G. Benettin and A. Ponno, “Time-Scales to Equipartition in the Fermi–Pasta–Ulam Problem: Finite-Size Effects and Thermodynamic Limit,” *Journal of Statistical Physics*, vol. 144, pp. 793–812, Aug. 2011.
- [35] G. Benettin, H. Christodoulidi, and A. Ponno, “The Fermi-Pasta-Ulam Problem and Its Underlying Integrable Dynamics,” *Journal of Statistical Physics*, vol. 152, pp. 195–212, July 2013.
- [36] G. Benettin, S. Pasquali, and A. Ponno, “The Fermi–Pasta–Ulam Problem and Its Underlying Integrable Dynamics: An Approach Through Lyapunov Exponents,” *Journal of Statistical Physics*, vol. 171, pp. 521–542, May 2018.
- [37] C. Danieli, D. K. Campbell, and S. Flach, “Intermittent many-body dynamics at equilibrium,” *Physical Review E*, vol. 95, p. 060202, June 2017.
- [38] C. Y. Lin, S. N. Cho, C. G. Goedde, and S. Lichter, “When Is a One-Dimensional Lattice Small?,” *Physical Review Letters*, vol. 82, no. 2, p. 4, 1999.
- [39] J. Ford, “Equipartition of Energy for Nonlinear Systems,” *Journal of Mathematical Physics*, vol. 2, pp. 387–393, May 1961.
- [40] M. Onorato, L. Vozella, D. Proment, and Y. V. Lvov, “Route to thermalization in the  $\alpha$ -Fermi–Pasta–Ulam system,” *Proceedings of the National Academy of Sciences*, vol. 112,

pp. 4208–4213, Apr. 2015.